Transient photoluminescence and simultaneous amplified spontaneous emission from multiexciton states in CdSe quantum dots

J.-Michel Caruge, Yinthai Chan, V. Sundar, H. J. Eisler, and Moungi G. Bawendi
Department of Chemistry, Massachusetts Institute of Technology, 77 Massachusetts Avenue, Cambridge, Massachusetts 02139, USA
(Received 28 January 2004; revised manuscript received 29 April 2004; published 27 August 2004)

We use transient photoluminescence to spectrally resolve the emission from 1, 2, and 3 electron-hole pairs states in CdSe colloidal quantum dots with radii ranging between 2.3 and 5.2 nm. The power dependence of the triexciton, biexciton and single exciton emission intensities are reported. We incorporate CdSe/ZnS core-shell nanocrystals into a TiO_2 host matrix and observe simultaneous amplified spontaneous emission from the $1S_{3/2}$-1Se and $1P_{3/2}$-$1P_e$ quantum dot transitions. The achievement of amplified spontaneous emission from the $1P_e$ QD state suggests that the $1P_e$ state sixfold degeneracy might be lifted by the e-h exchange interaction.

DOI: 10.1103/PhysRevB.70.085316 PACS number(s): 78.67.Bf, 78.55.Et, 73.21.−b, 73.22.Lp

I. INTRODUCTION

Over the past decade, multiexciton states in semiconductor quantum dots (QDs) have attracted the attention of many investigators. The discrete QD energy levels and the three dimensional (3D) quantum confinement of multiple carriers have been exploited, in epitaxially grown QDs, to produce strongly correlated photon pairs,[1] nonclassical optical field states[2] or to demonstrate the optical entanglement of excitons[3] in a QD.

The wet chemical synthesis of semiconductor QDs allows nanocrystal (NC) size and shape control[4–6] and enables an increase of the 3D quantum confinement of the electron and hole. Unlike in epitaxial QDs, fast nonradiative processes dominate multiexciton relaxation in strongly confined colloidal QDs. The Coulomb mediated Auger mechanism[7,8] has been proposed as the main nonradiative pathway for multiple carrier relaxation. In particular, for CdSe NCs, high-resolution time resolved experiments show that multiexciton dynamics depend strongly on the QD radius.[7] For instance, reducing the radius of spherical CdSe QDs from 4.2 to 2.3 nm decreases the biexciton Auger relaxation time by a factor of 8: from 360 ps to 42 ps.

Recently,[9] an ultra-fast photoluminescence (PL) up-conversion technique was used to detect multiexcitonic emission in CdSe colloidal QDs, and a charged biexciton model was introduced to explain the observed higher energy multiexcitonic band at high excitation power. In this article, we also report the observation of such a multiexcitonic band. We find, however, that its energy position and power dependence strongly suggest that this band originates from a 3 electron-hole (e-h) pair recombination. Moreover, we also show that the nonlinear excitation of CdSe/ZnS core-shell NCs embedded in a high volume fraction in a TiO_2 matrix gives rise to amplified spontaneous emission (ASE) from that multiexcitonic band.

II. EXPERIMENTS AND RESULTS

Highly luminescent CdSe NCs were prepared based on the method of Ref. 10 and dispersed in low concentration into hexane in a 1 mm length quartz cuvette. The bare CdSe NCs were excited by a frequency doubled regenerative titanium–sapphire amplifier, delivering 100 fs long pulses at 400 nm at a repetition rate of 1 kHz. Within our pump fluence, up to 10 e-h pairs could be injected into the QDs on average. The mean number of e-h pairs is given by

$$\bar{n} = \frac{\sigma \lambda P}{h c A} = \alpha P, \tag{1}$$

where σ, λ, h, c, A and P are the QD absorption cross-section[11] at 400 nm, the excitation wavelength, the Planck constant, the speed of light, the beam cross-sectional area and the pump power, respectively. The room temperature PL was collected with a 5 cm focal length lens, dispersed with a 100 grooves/mm grating and directly detected with a streak camera. The time resolution of the detection setup was 18 ps for the shortest experimental time range.

Figure 1(a) shows a three dimensional transient PL spectrum for a 2.3 nm radius CdSe QDs sample; 4 e-h pairs are injected into the QDs on average. The PL intensity is coded in a white color, brighter area corresponding to higher PL intensity. Figure 1(d) shows PL spectra, extracted from Fig. 1(a), 20 ps (star) and 800 ps (circle) after excitation using a 40 ps integration window. The transient PL spectra show that, shortly after excitation, a second emission peak is present at higher energy than the usual band edge emission peak. The higher energy band is only observed at high excitation power, which confirms its multiexcitonic origin. The splitting, Δ, between the two peaks is 0.25 eV in Fig. 1(b). Figure 1(c) shows that increasing the NC's radius from 2.3 nm to 4.3 nm decreases Δ by a factor of 2. We checked that the decrease observed in Δ is not mainly due to a significant variation of the band edge Stokes shift: we obtained band edge Stokes shifts between 10 and 25 meV for QDs radii ranging between 2.3 and 5.2 nm; that are consistent with nonresonant Stokes shift values reported by Kuno *et al.* in Ref. 12. Figure 1(d) displays the band edge emission spectrum for 2.3 nm radius QDs 20 ps (square) and 800 ps (triangle) after excitation. Since the band edge peak is a mixture of single and biexciton emission, the observed 20 meV positive energy shift with time is evidence for the negative bind-

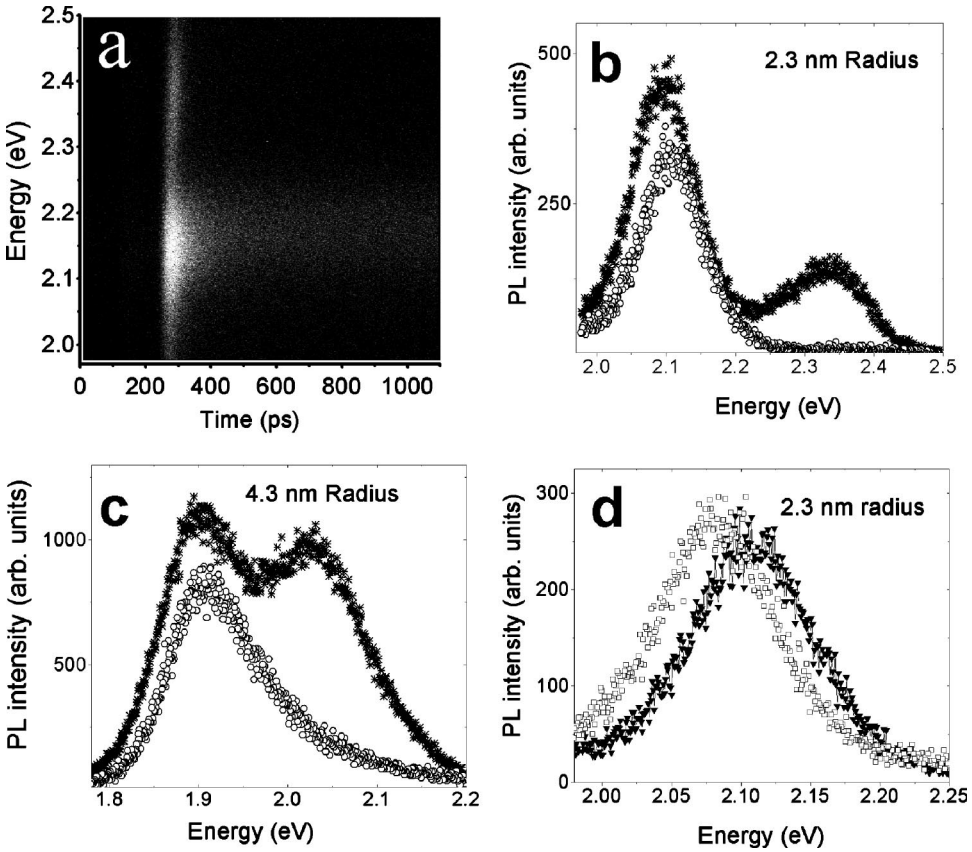

FIG. 1. (a) 3D transient PL spectrum recorded on a 1.1 ns timescale for a 2.3 nm radius QDs sample; the PL intensity is coded in white color; brighter area corresponds to higher PL intensity. (b) PL spectra 20 ps (stars) and 800 ps (circles) after excitation extracted from Fig. 1(a). (c) 4.3 nm QD radius PL spectra 20 ps (stars) and 800 ps (circles) after excitation. (d) 2.3 nm radius QD band edge PL spectra 60 ps (open triangle) and 800 ps (solid triangle) after excitation, the blue shift is due to negative biexciton binding energy.

ing energy of the biexciton as previously reported.[9] Figure 2(a) summarizes the evolution of Δ as a function of the NC size.

To determine the origin of the multiexcitonic band, we first compared the size evolution of Δ with single exciton absorption spectra of CdSe QDs, reported earlier by Norris *et al.*[13] Figure 2(b) compares Δ (squares) and the position of the $1P_{3/2}$-$1P_e$ transition (triangles) relative to the $1S_{3/2}$-$1S_e$ band edge transition. As the PLE data in Ref. 13 were obtained at low temperature.(10 K) we use the energy of the first excited state of our QD samples, instead of the QD size, to get the relative energy of the $1P_{3/2}$-$1P_e$ transition from Ref. 13. Indeed, one has to take into account the increase of the effective band gap of the QD with temperature.[14] For instance, the extracted 0.31 eV spacing for the 2.3 nm QDs sample [cf. Fig. 2(b)] is consistent with the room temperature value reported in Ref. 15. We also measured the position of the $1P_{3/2}$-$1P_e$ transition by performing room temperature lin-

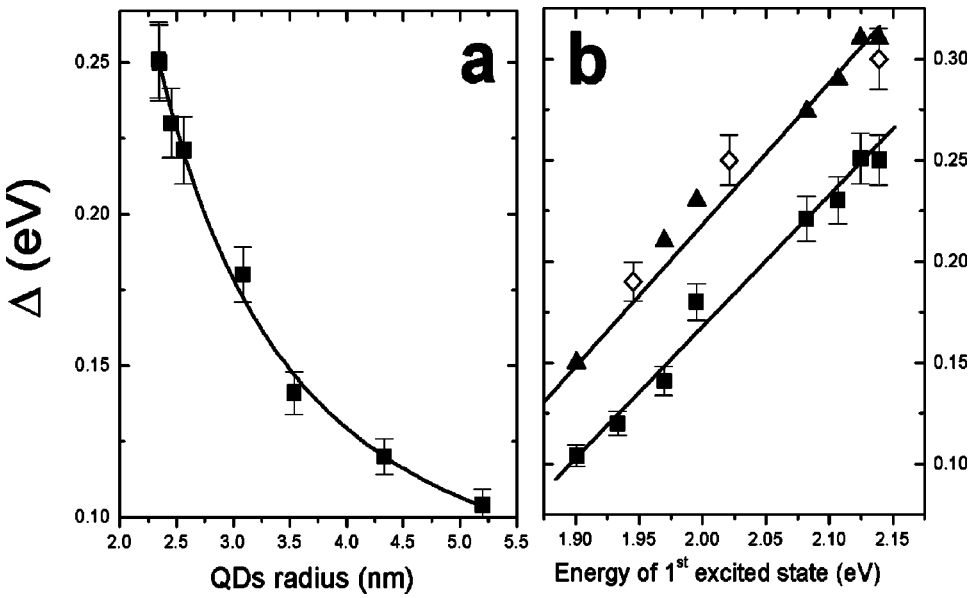

FIG. 2. (a) Δ versus the QD radius; (b) a comparison between Δ (squares) and the $1P_{3/2}$-$1P_e$ energy transition (triangles) relative to the $1S_{3/2}$-1Se band edge transition; the notation $1S_{3/2}$, $1P_{3/2}$, $1S_e$ and $1P_e$ of Ref. 20 designates the first two hole and electron levels, respectively; measured $1P_{3/2}$-$1P_e$ energy position (diamonds) for three QD samples at room temperature.

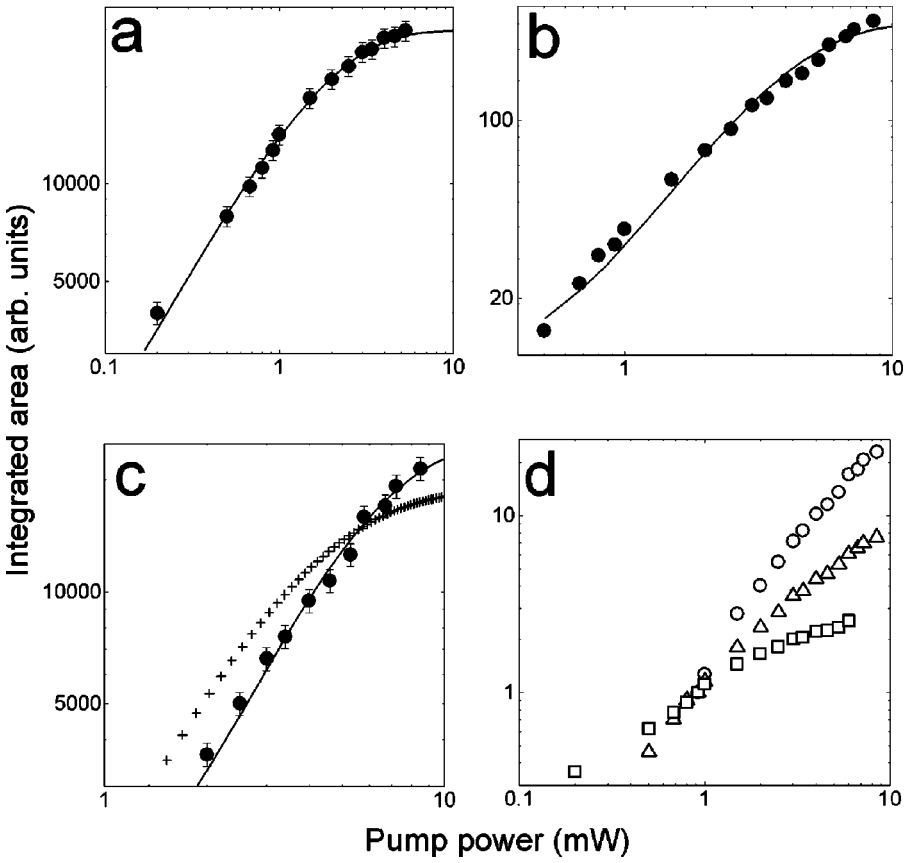

FIG. 3. (a) Single exciton saturation curve; single exciton spectra are taken 1 ns after excitation. Solid line (least square fit) shows that Eq. (2) reproduces the saturation curve. (b) Biexciton emission power dependence; the solid line shows the least square fit result using Eq. (3). (c) Multiexcitonic band power dependence (circles) and least square fit results using Eq. (3) (crosses) and Eq. (4) (solid line), respectively. (d) Normalized power dependence of the single exciton (squares) biexciton (triangles) and the multiexcitonic band (circles); the 3 different slopes show that the 3 bands originate from 3 different emission processes.

ear absorption measurements on three different QD samples [open diamonds in Fig. 2(b)] and obtained a good agreement between the low and room temperature data.

Within our size range, we obtain an approximately 50 meV energy difference between Δ and the relative position of the $1P_{3/2}$-$1P_e$ transition, a value that is different from the recently reported values.[9]

We further characterized the transient PL data by establishing the power dependence of each emission band. Figures 3(a)–3(c) present the power dependence of the single exciton, biexciton and the multiexcitonic band, respectively. The method for extracting the biexciton spectrum from the band edge emission spectrum is described in the next section. Figure 3(d) summarizes the power dependence of the three bands, normalized to their intensity at $P=1$ mW. The three different slopes suggest that the three bands originate from three different emission processes.

A further characterization of our transient PL data includes the determination of the relaxation time of each emission band. Figure 4(a) presents the dynamics, at high power, of the band edge emission peak for 3.4 nm (circles) and 2.3 nm (diamonds) radius CdSe QDs. As our measured single exciton lifetime is 14 ns, we assign the fast band edge dynamics, observed on a 1 ns timescale in Fig. 4(a), to biex-

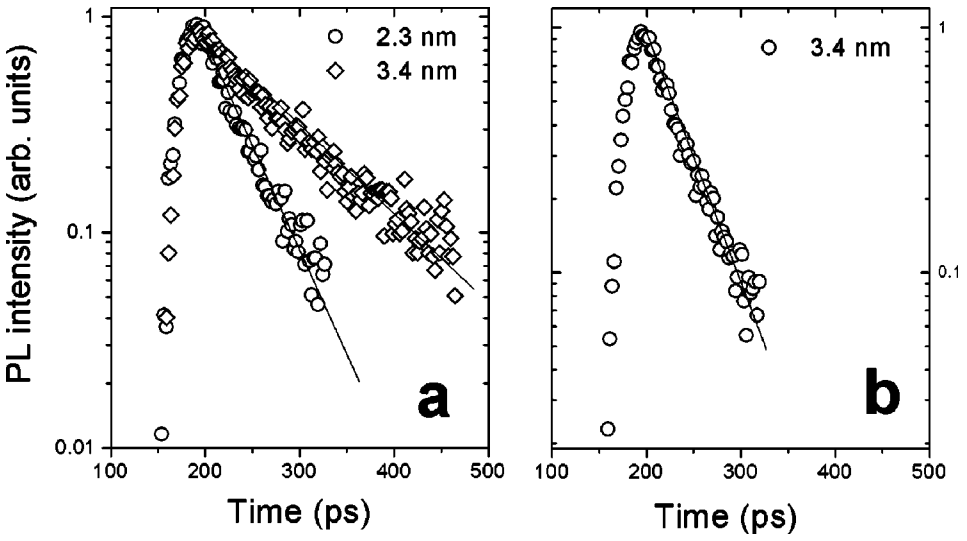

FIG. 4. (a) 2.3 nm (circles) and 3.4 nm (diamonds) radius QD biexciton PL decay curves. (b) PL decay curve (circles) of the multiexcitonic band for a 3.4 nm radius QD sample.

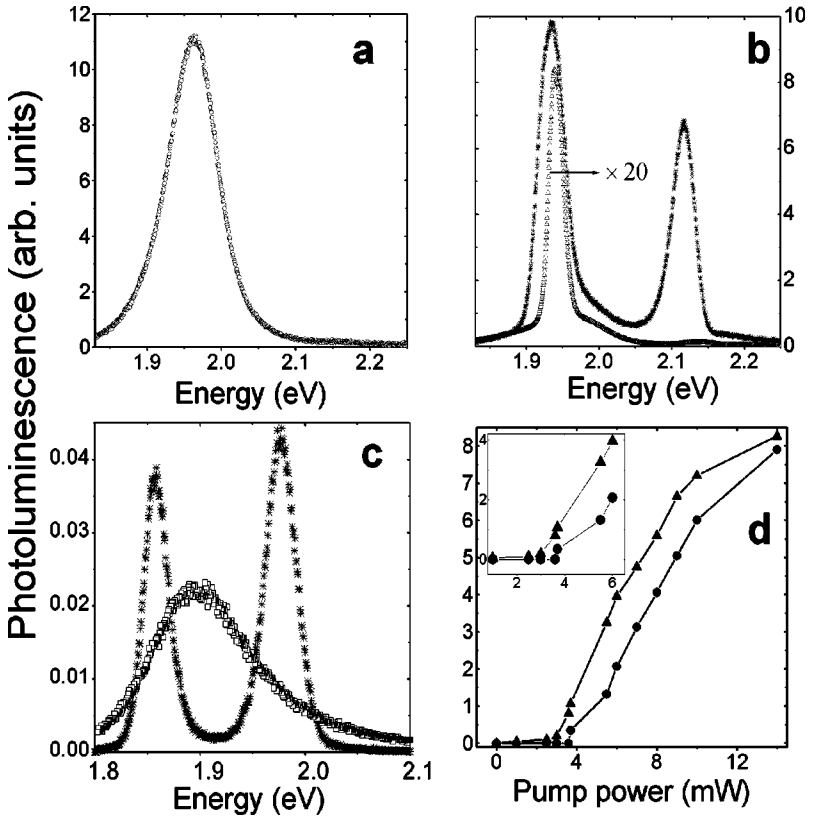

FIG. 5. (a) Linear PL spectrum of a 3.1 nm radius QD doped titania thin film. (b) PL spectrum for 2.2 e-h pairs injected on average into the QDs (triangles); simultaneous ASE (stars) for 4 e-h pairs injected on average into the QDs; FWHM for the two peaks are on the order of 30 meV (10 nm). (c) Power dependence of the integrated area under the first (triangle) and second peak (circle); the inset is a zoom around the threshold regions. (d) Simultaneous ASE (stars) for a 5.2 nm radius QDs doped titania thin film, the square curve represents the PL spectrum at low pump intensity.

citon relaxation. The measured biexciton lifetimes, τ_2, are 150 ps (3.4 nm QD radius) and 50 ps (2.3 nm radius QDs), consistent with previous reported values.[7,9] Figure 4(b) gives a 50 ps relaxation time for the multiexcitonic band for 3.4 nm radius QDs.

Finally, following Ref. 16, we use sol-gel processing to incorporate CdSe/ZnS core-shell NCs in a high volume fraction into TiO_2 thin films. A typical film refractive index and thickness as measured by ellipsometry are 1.7 and 250 nm and are tunable by varying the QDs concentration and the spin speed during the spin-coating process. The 400 nm excitation light is focused onto one of the faces of the device and the detected PL is spectrally analyzed with a CW CCD cooled camera. Figure 5(a) shows the linear PL spectrum of a TiO_2 thin film incorporating 3.1 nm radius CdSe/ZnS core-shell NCs. Above a first intensity threshold value we observed the usual biexciton ASE peak on the red side of the linear PL spectrum [triangles in Fig. 5(b)]. Increasing the pump power gives rise to a second, higher energy ASE peak [stars in Fig. 5(c)]. The position of the second ASE peak coincides with the position of the multiexcitonic band, observed in the transient PL spectrum. Figure 5(c) summarizes the evolution of the integrated area below the first (solid triangle) and second (solid circle) peak as a function of the pump power. The two distinct threshold values correspond to 2.2 and 4 e-h pairs injected on average into a NC. Figure 5(d) shows that the 2 ASE peaks, from both bands, are also observed for QDs with a larger radius (5.2 nm). Within our wave-guide optical confinement factor, simultaneous ASE was only observed for QDs with radii larger than 3.1 nm; ASE from the band edge transition, however, is preserved for QDs smaller than 3.1 nm.

III. ANALYSIS AND DISCUSSION

Our reported energy positions for the multiexcitonic band differ significantly from those reported in Ref. 9. For instance, the transient PL spectrum shown in Fig. 1(b) (stars) is similar to the spectrum reported in Ref. 9: a band edge and multiexcitonic emission peaks centered on 2.1 and 2.35 eV, respectively. The clear separation between the 2 peaks, in our transient PL spectrum, enables a straightforward evaluation of the energy position of the multiexciton band and the energy splitting Δ: 2.35 and 0.25 eV, respectively. The size evolution of Δ, in Figs. 2(a) and 2(b), is further supported by our simultaneous ASE data. Indeed, the energy spacing between the 2 narrow ($\approx$10 nm FWHM) ASE peaks is 0.18 eV and 0.12 eV for 3.1 and 5.2 nm QD radius, in good agreement with the values reported in Figs. 2(a) and 2(b). We therefore believe that our energy positions are accurate.

The correlation between Δ and the $1P_{3/2}$-$1P_e$ energy transition [Figs. 2(a) and 2(b)] suggests that the multiexcitonic band originates from a 3 e-h pair state: 2 electrons in the first 1Se electronic state, 2 holes in the first $1S_{3/2}$ state, a third electron in the next $1P_e$ electronic state and a third hole in the $1P_{3/2}$ state. The 50 meV energy offset between Δ and the relative position of the $1P_{3/2}$-$1P_e$ transition may result from the triexciton binding energy and a Stokes shift due to the fine structure of the $1P_{3/2}$-$1P_e$ QD transition.

We now validate this hypothesis by analyzing the power dependence of the single exciton, biexciton and the multiexcitonic band for the 2.3 nm QD sample. We assume a Poisson distribution $p(n)=\overline{n}^n e^{-\overline{n}}/n!$ for the number, n, of e-h pairs injected into a QD after a short excitation pulse; where $\overline{n}$ is given by Eq. (1).

The single exciton PL intensity at time $t \gg \tau_2$ (τ_2 is the biexciton lifetime) is proportional to the probability of generating more than 0 e-h pairs per QD immediately after the excitation pulse. The single exciton PL intensity, $I_1(P)$, is therefore given by

$$I_1(P) = C_1(1 - p(0)) = C_1(1 - e^{-\alpha P}), \tag{2}$$

where C_1 and α are two fitting parameters. The solid line in Fig. 3(a) shows that Eq. (2) closely reproduces the saturation curve of the single exciton for the 2.3 nm QD sample. The fit gives $\alpha = 0.56$, which leads to an absorption cross-section [using (1) with $A = 0.032$ cm^2] $\sigma = 6 \times 10^{-15}$ cm^2, consistent with the 5×10^{-15}cm^2 value reported in Ref. 11.

Since the multiexcitonic band is well separated from the band edge emission peak [Figs. 1(a) and 1(b)], we can directly obtain its power dependence by obtaining its time-integrated area during a 1 ns window. To minimize errors due to the weak overlap between the two peaks, we use a 10 nm (25 meV) integration window on the blue side (higher energy side) of the emission peak. Then, we first assume, as in Ref. 9, that the band originates from a charged biexciton. The time integrated PL intensity, $I_2(P)$, should then be proportional to the probability of generating more than 1 e-h pair per dots after each excitation pulse:

$$I_2(P) = C_2\{1 - p(0) - p(1)\} = C_2\{1 - (1 + \alpha P) \times e^{-\alpha P}\}, \tag{3}$$

where C_2 is the only fitting parameter and α has been previously determined from the single exciton saturation curve. As illustrated by the crosses in Fig. 3(c), Eq. (3) does not fit the power dependence of the multiexcitonic band.

We therefore consider a 3 e-h pair recombination mechanism. The time integrated PL intensity is then given by

$$\begin{aligned} I_2(P) &= C_3(1 - p(0) - p(1) - p(2)) \\ &= C_3\left[1 - \left(1 + \alpha P + \frac{\alpha^2 P^2}{2!}\right) \times e^{-\alpha P}\right], \end{aligned} \tag{4}$$

where C_3 is the only fitting parameter. Equation (4) closely reproduces the power dependence of the emission peak as shown by the solid line in Fig. 3(c). We therefore conclude that the multiexcitonic band originates from a 3 e-h pair emission process.

Next, we derive the biexciton PL spectrum and its power dependence. As the band edge emission peak is a mixture of biexciton and single exciton emission, we must subtract a single exciton contribution from the band edge PL spectrum at time $t \leqslant \tau_2$. Indeed, as the biexciton lifetime for a 2.3 nm QD sample is 50 ps [Fig. 4(b)], only a small portion of the initial biexciton population will contribute to the single exciton spectrum at time $t = 1$ ps, for instance. This fraction is given by $1 - \exp(-1/50) = 0.02$ (2%). At time $t = 20$ ps this fraction is 32%. Therefore, we calculate the evolution of the single exciton population as a function of time and pump power. To achieve this goal, the following linear set of equations for the N e-h pair population needs to be solved.

Let f_N be the N e-h pair population inside a QD, at time t; then

$$\frac{df_N}{dt} = \Gamma_{N+1} f_{N+1} - \Gamma_N f_N,$$

$$\sum_N f_N = 1, \tag{5}$$

where Γ_N is the N e-h pair relaxation rate. Initial conditions for the linear set of equations are $f_N(t=0) = p(N)$. We then make the following approximation: We limit our calculation to a maximum number of 3 e-h pairs and modify the initial condition for the triexciton population to $f_3(t=0) \approx p(3) + p(4) + \cdots$. This approximation holds for $\Gamma_4 \gg \Gamma_3$ and/or at a moderate pump power, i.e., at a low probability of injecting more than 3 e-h pairs into a QD. Equation (5) is then solved to yield the following expression for the single exciton population:

$$f_1(t) = Ae^{-\Gamma_1 t} + Be^{-\Gamma_2 t} + Ce^{-\Gamma_3 t},$$

$$C = \frac{\Gamma_2 \Gamma_3 p(3)}{(\Gamma_1 - \Gamma_3)(\Gamma_2 - \Gamma_3)}, \quad B = \frac{\Gamma_2}{\Gamma_2 - \Gamma_1}\left[p(2) + \frac{\Gamma_3 p(3)}{\Gamma_3 - \Gamma_2}\right],$$

$$A = p(1) - B - C.$$

.

We can then calculate the contribution of the single exciton to the band edge PL spectrum at time t by rescaling the band edge spectrum obtained at time $t_1 \gg \tau_2$ by the ratio $f_1(t)/f_1(t_1)$.

Figure 6(a) (circles) shows the transient PL spectrum obtained 20 ps after excitation for the 2.3 nm QD sample. The solid line in Fig. 6(a) shows the same PL spectrum after subtraction of the single exciton contribution: the peaks correspond to the biexciton and triexciton emission bands. We plot in Fig. 6(b) the single exciton contribution to the PL spectrum at time $t = 20$ ps (diamonds) and 300 ps (circles). At 300 ps we retrieve the saturation curve of the single exciton. At shorter time, the single exciton contribution saturates and decays. The drop is due to the expected "Poissonian decay" [crosses in Fig. 6(b)] of the probability to generate 1 e-h pair per QD right after the excitation pulse. The difference between the expected (crosses) and observed (diamonds) decays results from relaxation of multiexciton states. Finally, the power dependence of the biexciton is obtained by plotting the integrated area under the calculated biexciton emission peak. The solid line in Fig. 3(b) shows that Eq. (3) approximately reproduces the power dependence of the biexciton, which validates, for this QD sample, the approximations made.

The energy positions combined with the power dependence of the multiexcitonic band lead us to conclude that this band is due to a triexciton recombination process from the $1P_{3/2}$-1Pe QD transition. However, as the intraband relaxations of holes and electrons take place on a subpicosecond timescale[17,18] (faster than the triexciton lifetime) a hole in the $1P_{3/2}$ state should quickly relax to the lowest $1S_{3/2}$ state. As the annihilation of a 1P electron and a 1S hole is theoreti-

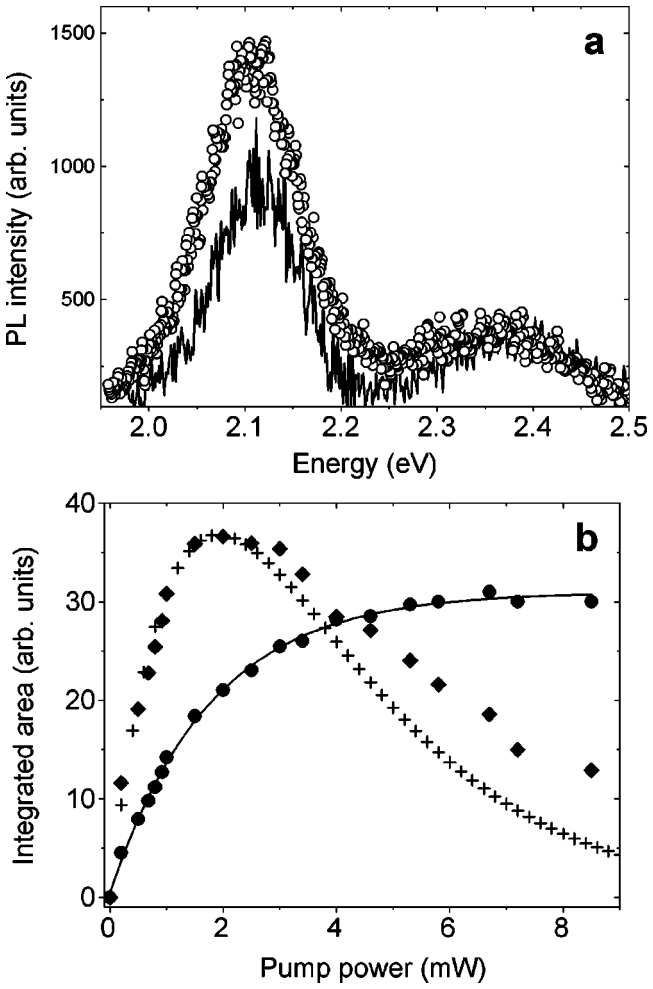

FIG. 6. (a) PL spectra 20 ps after excitation before (stars) and after (circles) subtraction of the single excitation contribution. (b) Contribution of the single exciton emission to the PL spectrum 20 ps (diamonds) and 300 ps (circles) after excitation and rescaled Poissonian probability (crosses) to generate more than 1 e-h pair per QD right after an excitation pulse.

cally forbidden the triexciton emission should not be detected. We propose two mechanisms to explain the observation of the triexciton emission peak.

Firstly the e-h Coulombic interaction mixes the electron and hole states[19] and as a result alters the selection rules for the electric dipole transition. The $1P_e$-$1S_h$ relaxation, previously forbidden, can therefore be allowed. Second, previous calculations[20] and two-photon excitation[21] of CdSe QDs show that the $1P_{3/2}$ hole state is positioned (within our experimental QD size range) approximately 15 meV higher than the lowest $1S_{3/2}$ hole state. This energy spacing is less than the thermal energy (25 meV at 300 K) so that the triexciton emission could occur through the thermal population of the $1P_{3/2}$ hole state. Consistent with this prediction, cooling a 2.3 nm radius QD sample to 77 K results in a significant decrease of the triexciton PL intensity.

The observation of ASE from the triexciton emission band is surprising. Indeed, because of the high degeneracy of the $1P_e$ electronic state, one might not expect to observe ASE from the $1P_{3/2}$-$1P_e$ QD transition. We speculate that the e-h exchange interaction, which plays an important role in the strong confinement regime,[22] partially lifts the degeneracy of the $1P_e$ electronic state. The exchange interaction should lift the degeneracy by splitting the $1P_e$ levels into different sublevels with spin 0, 1, 2 and 3. Furthermore, the observation of ASE from the triexciton emission band is only possible if the ASE build up time is shorter than the optical gain relaxation time,[23] which is dominated by the $N \geqslant 3$ e-h pairs damping rate. The ASE build up time is related to the QD loading fraction and the optical confinement factor of the wave-guiding media. We therefore speculate that our inability to observed ASE from the triexciton band for QDs with radii smaller than 3.1 nm is due to their faster optical gain relaxation. Increasing the QD loading fraction, the monodispersity of the QD sample and use of higher quality factor microcavities should allow the observation of ASE from the multiexcitonic band of QDs smaller than 3.1 nm in radius.

IV. CONCLUSION

In summary, using simple transient PL measurements, we show that the multiexcitonic band observed on the blue side of the band edge emission peak in CdSe nanocrystal QDs, under high excitation power, originates from a triexciton recombination. The triexciton emission may be thermally assisted and/or facilitated by e-h Coulombic interaction. Possible implications of this work include the generation of highly correlated photon pairs or triplets from single CdSe NCs, a transition from antibunching to bunching of photons on a 100 ps or ns timescale and multistate lasing in QD doped photonic devices.

ACKNOWLEDGMENTS

This work was supported in part by the NSF-MRSEC program, the David and Lucile Packard Foundation and by the Department of Energy. We also thank J. Hodgkiss for technical assistance with the laser and detection systems.

[1] E. Moreau, I. Robert, L. Manin, V. Thierry-Mieg, J. M. Gerard, and I. Abram, Phys. Rev. Lett. **87**, 183601 (2001).
[2] O. Benson, C. Santori, M. Pelton, and Y. Yamamoto, Phys. Rev. Lett. **84**, 2513 (2000).
[3] G. Chen, N. H. Bonadeo, D. G. Steel, D. Gammon, D. S. Katzer, D. Park, and L. J. Sham, Science **289**, 1906 (2000).
[4] C. B. Murray, D. J. Norris, and M. G. Bawendi, J. Am. Chem. Soc. **115**, 8706 (1993).
[5] X. Peng, L. Manna, W. Yang, J. Wickham, E. Scher, A. Kadavanich, and A. P. Alivisatos, Nature (London) **404**, 59 (2000).
[6] X. Peng, Adv. Mater. (Weinheim, Ger.) **15**, 459 (2003).
[7] V. Klimov, A. A. Mikhailovsky, D. W. McBranch, C. A.

Leatherdale, and M. G. Bawendi, Science **287**, 1011 (2000).
[8] V. A. Kharchenko and M. Rosen, J. Lumin. **70**, 158 (1996).
[9] M. Achermann, J. A. Hollingsworth, and V. I. Klimov, Phys. Rev. B **68**, 245302 (2003).
[10] B. R. Fisher, H. J. Eisler, N. E. Stott, and M. G. Bawendi, J. Phys. Chem. B **108**, 143 (2004) (supplemental information).
[11] C. A. Leatherdale, W.-K. Woo, F. V. Mikulec, and M. G. Bawendi, J. Phys. Chem. B **106**, 7619 (2002).
[12] M. Kuno, J. K. Lee, B. O. Dabbousi, F. V. Mikulec, and M. G. Bawendi, J. Chem. Phys. **106**, 9869 (1997).
[13] D. J. Norris and M. G. Bawendi, Phys. Rev. B **53**, 16338 (1996).
[14] T. Vossmeyer, L. Katsikas, M. Giersig, I. G. Popovic, K. Diesner, A. Chemseddine, A. Eychmuller, and H. Weller, J. Phys. Chem. **98**, 7665 (1994).
[15] P. Guyot-Sionnest and M. A. Hines, Appl. Phys. Lett. **72**, 686 (1997).
[16] V. Sundar, H. J. Heisler, and M. G. Bawendi, Adv. Mater. (Weinheim, Ger.) **14**, 739 (2002).
[17] V. Klimov, A. A. Mikhailovsky, D. W. McBranch, C. A. Leatherdale, and M. G. Bawendi, Phys. Rev. B **61**, R13349 (2000).
[18] U. Woggon, H. Giessen, F. Gindele, O. Wind, B. Fluegel, and N. Peyghambarian, Phys. Rev. B **54**, 17681 (1996).
[19] S. H. Park, R. A. Morgan, Y. Z. Lindberg, S. W. Koch, and N. Peyghambarian, J. Opt. Soc. Am. B **7**, 2097 (1990).
[20] A. I. Ekimov, F. Hache, M. C. Shanne-Klein, D. Ricard, C. Flytzanis, I. A. Kudryavtsev, T. V. Yazeva, A. V. Rodina, and Al. L. Efros, J. Opt. Soc. Am. B **10**, 100 (1993).
[21] S. A. Blanton, M. A. Hines, M. E. Schmidt, and P. Guyot-Sionnest, J. Lumin. **70**, 253 (1996).
[22] Al. L. Efros, M. Rosen, M. Kuno, M. Nirmal, D. J. Norris, and M. Bawendi, Phys. Rev. B **54**, 4843 (1996).
[23] V. I. Klimov, A. A. Mikhailovsky, Su Xu, A. Malko, J. A. Hollingsworth, C. A. Leatherdale, H. J. Eisler, and M. G. Bawendi, Science **290**, 314 (2000).